Cellular/Molecular

Parvalbumin Is a Mobile Presynaptic Ca^{2+} Buffer in the Calyx of Held that Accelerates the Decay of Ca^{2+} and Short-Term Facilitation

Martin Müller,[1,2] **Felix Felmy,**[3] **Beat Schwaller,**[4] **and Ralf Schneggenburger**[1]

[1]Laboratory of Synaptic Mechanisms, Brain-Mind Institute, École Polytechnique Fédérale de Lausanne, 1015 Lausanne, Switzerland, [2]Graduate School of Neural and Behavioral Sciences, Universität Tübingen, 72074 Tübingen, Germany, [3]Biology II, Department for Neurobiology, Ludwig-Maximilians-University, 82152 Martinsried, Germany, and [4]Unit of Anatomy, Department of Medicine, University of Fribourg, 1705 Fribourg, Switzerland

Presynaptic Ca^{2+} signaling plays a crucial role in short-term plasticity of synaptic transmission. Here, we studied the role of mobile endogenous presynaptic Ca^{2+} buffer(s) in modulating paired-pulse facilitation at a large excitatory nerve terminal in the auditory brainstem, the calyx of Held. To do so, we assessed the effect of presynaptic whole-cell recording, which should lead to the diffusional loss of endogenous mobile Ca^{2+} buffers, on paired-pulse facilitation and on intracellular Ca^{2+} concentration ($[Ca^{2+}]_i$) transients evoked by action potentials. In unperturbed calyces briefly preloaded with the Ca^{2+} indicator fura-6F, the $[Ca^{2+}]_i$ transient decayed surprisingly fast (τ_{fast}, ~30 ms). Presynaptic whole-cell recordings made without additional Ca^{2+} buffers slowed the decay kinetics of $[Ca^{2+}]_i$ and paired-pulse facilitation (twofold to threefold), but the amplitude of the $[Ca^{2+}]_i$ transient was changed only marginally. The fast $[Ca^{2+}]_i$ decay was restored by adding the slow Ca^{2+} buffer EGTA (50–100 μM) or parvalbumin (100 μM), a Ca^{2+}-binding protein with slow Ca^{2+}-binding kinetics, to the presynaptic pipette solution. In contrast, the fast Ca^{2+} buffer fura-2 strongly reduced the amplitude of the $[Ca^{2+}]_i$ transient and slowed its decay, suggesting that the mobile endogenous buffer in calyces of Held has slow, rather than fast, binding kinetics. In parvalbumin knock-out mice, the decay of $[Ca^{2+}]_i$ and facilitation was slowed approximately twofold compared with wild-type mice, similar to what is observed during whole-cell recordings in rat calyces of Held. Thus, in young calyces of Held, a mobile Ca^{2+} buffer with slow binding kinetics, primarily represented by parvalbumin, accelerates the decay of spatially averaged $[Ca^{2+}]_i$ and paired-pulse facilitation.

Key words: synaptic transmission; Ca^{2+}; facilitation; short-term plasticity; Ca^{2+}-binding protein; nerve terminal

Introduction

Synapses are capable of relaying signals in a highly dynamic manner, depending strongly on their recent history of activity. Facilitation of transmitter release is possibly the shortest form of synaptic plasticity (duration, ~100 ms), caused by a transient elevation of residual Ca^{2+} in the nerve terminal that enhances the release probability during a subsequent action potential (AP) (Zucker and Regehr, 2002). Because residual Ca^{2+} causes facilitation, it is likely that endogenous Ca^{2+} buffers in nerve terminals modulate facilitation. The effects of a given Ca^{2+} buffer on the intracellular Ca^{2+} concentration ($[Ca^{2+}]_i$) transients are determined by the affinity of the buffer for Ca^{2+} and by its Ca^{2+}-binding kinetics. Calbindin D-28k, a Ca^{2+}-binding protein with relatively fast binding kinetics (Nägerl et al., 2000), reduces the

amplitude of spatially averaged $[Ca^{2+}]_i$ transients and concomitantly prolongs the decay of $[Ca^{2+}]_i$ (Airaksinen et al., 1997; Schmidt et al., 2003b), as predicted by "single-compartment models" of cellular Ca^{2+} signaling for Ca^{2+} buffers with fast binding kinetics (Neher and Augustine, 1992; Helmchen et al., 1997). Fast endogenous mobile buffers can also interfere with the "local" Ca^{2+} signal relevant for vesicle fusion (Edmonds et al., 2000), and (partial) saturation of fast Ca^{2+} buffers during an increase of residual Ca^{2+} is thought to contribute to transmitter release facilitation at some synapses ["buffer saturation mechanism" (Neher, 1998; Blatow et al., 2003; Felmy et al., 2003; Matveev et al., 2004)]. In contrast, Ca^{2+}-binding proteins with slow binding kinetics, such as parvalbumin, do not significantly reduce the peak amplitude of $[Ca^{2+}]_i$ but rather accelerate the initial decay of $[Ca^{2+}]_i$ (Lee et al., 2000; Collin et al., 2005). Thus, by differentially shaping the amplitude and/or the decay of the presynaptic $[Ca^{2+}]_i$ transient, different Ca^{2+}-binding proteins likely modulate facilitation of transmitter release in specific ways.

The calyx of Held is a large glutamatergic synapse in the auditory brainstem, at which direct whole-cell recordings can be made from the presynaptic nerve terminal (Forsythe, 1994; Borst et al., 1995). This synapse exhibits depression during high-frequency trains, but lowering the release probability uncovers

facilitation (Borst et al., 1995; Felmy et al., 2003). The endogenous Ca^{2+} buffers that govern Ca^{2+} signaling and facilitation of transmitter release at the calyx of Held are, however, not well identified. Using a fura-2 overload method, Helmchen et al. (1997) estimated that the calyx of Held has a low endogenous buffer capacity (κ_S) of ~40, which probably represents the activity of endogenous immobile Ca^{2+} buffers, as has been shown in chromaffin cells (Xu et al., 1997). In addition, calyces of Held might also have mobile endogenous Ca^{2+} buffer(s). By monitoring the effects of the presynaptically added Ca^{2+} buffers EGTA and BAPTA on transmitter release, Borst and Sakmann (1996) inferred that calyces of Held contain a low concentration of mobile endogenous Ca^{2+} buffers, equivalent to ~200 μM EGTA or 50 μM BAPTA. Studying the mechanism of short-term facilitation at the calyx of Held, Felmy et al. (2003) suggested that a Ca^{2+} buffer with fast binding kinetics might act as a saturable buffer in synaptic facilitation. However, the molecular identity, Ca^{2+}-binding kinetics, and functional role of mobile endogenous Ca^{2+} buffer(s) at the calyx of Held have remained elusive, although it has been shown by immunohistochemistry that calyces of Held express parvalbumin, and, at later stages of development, also calretinin (Felmy and Schneggenburger, 2004).

Here, we investigated how mobile endogenous Ca^{2+} buffers influence Ca^{2+} signaling and paired-pulse facilitation at the calyx of Held. We show that a mobile Ca^{2+} buffer with slow Ca^{2+}-binding kinetics, mostly represented by parvalbumin, accelerates the decay of presynaptic [Ca^{2+}]$_i$ and short-term facilitation at this large excitatory nerve terminal.

Materials and Methods

Slice preparation and solutions. Transverse brainstem slices of 180–200 μm thickness were prepared with a Leica VT 1000 slicer, using postnatal day 8 (P8) to P10 Wistar rats, wild-type mice of the C57Bl/6J strain, and parvalbumin knock-out (PV−/−) mice (on the same C57Bl/6J background). The extracellular solution contained the following (in mM): 125 NaCl, 25 NaHCO$_3$, 2.5 KCl, 1.25 NaH$_2$PO$_4$, 25 glucose, 1 MgCl$_2$, 2 CaCl$_2$ (0.6 CaCl$_2$ in the case of afferent fiber stimulation experiments) (see Figs. 3, 6), 0.4 ascorbic acid, 3 myo-inositol and 2 Na-pyruvate, ~320 mOsm, pH 7.4, when bubbled with 95% O$_2$/5% CO$_2$. During simultaneous presynaptic and postsynaptic recordings (see Fig. 4), 10 mM TEA, 1 μM tetrodotoxin, and 50 μM D-2-amino-5-phophonovaleric acid were also present. The pipette solution for postsynaptic recordings contained the following (in mM): 135 Cs-gluconate, 20 tetraethylammoniumchloride, 10 HEPES, 5 Na$_2$-phosphocreatine, 4 MgATP, 0.3 Na$_2$GTP, and 5 EGTA. For the presynaptic recordings shown in Figure 4 (voltage clamp), the same solution was used without added Ca^{2+} buffer (see Fig. 4*A*) or with one of the following (combinations of) Ca^{2+} buffers: 100 μM EGTA (or 75 μM in a few cases) (see Fig. 4*B*), 100 μM fura-6F (see Fig. 4*C*), 100 μM fura-6F and 75 μM EGTA (see Fig. 4*D*), or 50 μM fura-2 (see Fig. 4*E*). For presynaptic current-clamp recordings or for brief preloading of fura-6F (see Figs. 1, 2, 5), the pipette solutions contained the following (in mM) 145 K-gluconate, 10 HEPES, 2 ATP-Mg, 0.3 Na$_2$GTP, 20 KCl, to which different concentrations of fura-6F, or fura-2 (see below), EGTA (100 μM), or rat recombinant parvalbumin (50 or 100 μM) were added. For the parvalbumin-loading experiments (see Fig. 2*C*), a 300 μg aliquot of lyophilized recombinant rat parvalbumin (>95% purity; molecular weight, 11,925 Da) was reconstituted with K-gluconate pipette solution on the day of the experiment. To facilitate seal formation, the pipette tip was first immersed in intracellular solution without parvalbumin for ~20–30 s and subsequently backfilled with parvalbumin-containing intracellular solution. Therefore, it is likely that the parvalbumin concentration at the tip of the patch pipette was lower than the nominal concentrations after reconstitution used here (50 and 100 μM; see Discussion). All experiments were performed at room temperature (20–25°C).

Whole-cell recordings were performed on presynaptic calyces and/or postsynaptic principal neurons of the medial nucleus of the trapezoid body, with an EPC-9/2 patch-clamp amplifier (HEKA Elektronik, Lambrecht/Pfalz, Germany). Series resistances (R_s) of postsynaptic recordings ranged from 3 to 8 MΩ (compensation up to 90%). EPSC traces were corrected for the remaining R_s error off-line. In presynaptic recordings, R_s was 15–30 MΩ (55% compensation). Presynaptic Ca^{2+} currents (see Fig. 4) are shown after P/5 correction. For current-clamp recordings, the fast current-clamp mode of the EPC-9 was used. Cells were visualized using an upright microscope (Olympus, Hamburg, Germany) equipped with infrared Dodt-gradient contrast illumination (Luigs and Neumann, Ratingen, Germany). For afferent fiber stimulation, presynaptic axons were stimulated with a concentric, bipolar stimulation electrode (MCE-100; Rhodes Medical Instruments, Woodland Hills, CA) as described previously (Meyer et al., 2001). During simultaneous presynaptic and postsynaptic recordings, we stimulated the terminals by short (0.6–1.2 ms) identical voltage-clamp depolarizations from −80 to +28 mV. The length of the pulses was adjusted in each cell pair such that the resulting EPSC amplitudes were 1–2 nA (see Fig. 4).

The amplitude and decay kinetics of paired-pulse facilitation was assessed by applying pairs of pulses at various interstimulus intervals (Δt) to the afferent fibers (see Figs. 3, 6) or to the voltage-clamped presynaptic terminal (see Fig. 4). During one trial, we applied paired pulses of all Δt (4 up to 400 ms) in a pseudorandomized sequence, applying pulse pairs every 5 s. Because of slight cumulative depression of the initial EPSC amplitude after the first stimulus, the first EPSC pair of each trial was discarded and repeated at the end of the trial. For analysis, we only considered trials in which the initial EPSC amplitudes ranged from 0.5 to 2.5 nA. Facilitation at any given Δt was calculated as the mean of all second EPSCs, divided by the mean of all first EPSCs (Kim and Alger, 2001), and expressed as: facilitation = mean EPSC2/mean EPSC1 × 100 (%).

Presynaptic Ca^{2+} imaging. Fura-6F (100 μM) or fura-2 (50 μM; both from Invitrogen, Eugene, OR) were added to the K-gluconate solution (see Figs. 1, 2, 5) or to the Cs-based presynaptic pipette solution (see above) to image [Ca^{2+}]$_i$ during continuous presynaptic whole-cell recordings. For brief preloading of a calyx of Held with ~80–100 μM fura-6F (see Figs. 1, 5), a whole-cell recording was made using 300 μM (or sometimes 400 μM) fura-6F. After 25–50 s (depending on R_s), the whole-cell recording was discontinued by gently withdrawing the patch pipette. This led to the preloading of ~80–100 μM fura-6F into the presynaptic terminal, as estimated by comparing the fluorescence intensities at the Ca^{2+}-independent excitation wavelength of 355 nm (F_{355}) with those recorded during subsequent continuous whole-cell recordings with 100 μM fura-6F.

The Ca^{2+}-imaging system (TILL-Photonics, Gräfelfing, Germany) used a monochromator to excite fura-6F at 355 and 380 nm and a 12-bit CCD camera. Pixel binning was 8 × 15 pixels (on-chip binning), allowing brief exposure times (5 ms). The illumination protocol (see Fig. 1*B*) consisted of 10 fluorescence ratio images (F_{355}/F_{380}) taken before the AP stimulus. Shortly (~100 ms) before and until ~1000 ms after the AP stimulus, only the Ca^{2+}-sensitive fluorescence at 380 nm was measured, allowing a higher sampling rate around the peak of the [Ca^{2+}]$_i$ signal (~140 Hz; 5 ms exposure, and 2 ms rest time between each F_{380} image). At the end of each protocol, another 10 ratio images were acquired. The values of F_{355} during the stimulus were obtained by linear interpolation of the measured F_{355} values before and after the stimulus (see Fig. 1*B*, dotted black line). During off-line analysis, the fluorescence values from $n = 6$ superpixels were read out (see Fig. 1*A*), and the background fluorescence was subtracted. The fluorescence ratio F_{355}/F_{380} was then calculated, using the measured (or interpolated) values of F_{355}. The ratio was converted into the intracellular free Ca^{2+} concentration ([Ca^{2+}]$_i$) using the equation given by Grynkiewicz et al. (1985).

The [Ca^{2+}]$_i$ traces in response to single APs measured with fura-6F (see Figs. 1*C1*,*D1*, 2*A–C*, 4*C*,*D*, 5*A*,*B*) are averages of 18–38 trials, which were separated by ~20 s. The decay of the resulting average [Ca^{2+}]$_i$ transient was fitted with single- and double-exponential functions. The fit was considered biexponential if both the ratio of the two time constants was more than two and if the amplitude of each exponential component contributed ≥15% to the total amplitude. Although most

[Ca^{2+}]$_i$ transients required biexponential fits, the relatively low signal-to-noise ratio of fura-6F imaging did not allow us to derive detailed information on the amplitude and time constants of the slow component of the [Ca^{2+}]$_i$ decay. The amplitude of [Ca^{2+}]$_i$ was calculated as the difference between two data points close to the maximum, and the average of 20 points before stimulus onset.

The calibration constants and the Ca^{2+}-binding properties of the indicator dye were determined in a combined *in vitro/in vivo* calibration approach (Schneggenburger, 2004). First, we measured the fluorescence spectra (340–380 nm) of fura-6F and fura-2 *in vitro* using thin quartz-glass capillaries (50 μm path length; In-vitroCom, Mountain Lakes, NJ) at different buffered [Ca^{2+}], using EGTA (for the lowest [Ca^{2+}]) and DPTA (1,3-diamino-2-propanol-*N*,*N*,*N'*,*N'*,-tetraacetic acid) as Ca^{2+} buffers. After normalizing the spectra to their fluorescence values at the isosbestic wavelength ($\sim$355 nm for fura-6F and $\sim$360 nm for fura-2), the apparent K_d of fura-6F (14.7 $\pm$ 0.6 μM [Ca^{2+}]; $n = 6$ calibrations), and fura-2 (0.2 μM; $n = 1$ calibration) for Ca^{2+} was analyzed using the Ca^{2+}-bound fraction of fura-6F at various [Ca^{2+}] (Schneggenburger, 2004). The apparent Ca^{2+} affinity of fura-6F (K_d, $\sim$15 μM) is somewhat lower than the one provided by the manufacturer (Invitrogen). The calibration constants for calculating the intracellular free Ca^{2+} concentration ([Ca^{2+}]$_i$) from the measured fluorescence ratio were measured in calyces of Held as described previously (Schneggenburger, 2004). The limiting fluorescence ratio at high [Ca^{2+}] (10 mM; R_{max}) was taken from *in vitro* measurements.

Effect of fura-6F on Ca^{2+} transients. Considering the apparent affinity of fura-6F for Ca^{2+} (K_d, 15 μM) and its estimated intracellular concentration achieved after preloading (80–100 μM; see above), we estimated the effect of fura-6F on the kinetics of [Ca^{2+}]$_i$ in the calyx of Held. Within the framework of the single-compartment model of Ca^{2+} signaling (Neher and Augustine, 1992; Helmchen et al., 1997), the time constant of [Ca^{2+}]$_i$ decay is given by the following: $\tau = 1/\gamma \times (1 + \kappa_S + \kappa_B)$, where γ is the lumped rate of Ca^{2+} extrusion across the plasma membrane and into organelles, κ_S is the endogenous Ca^{2+}-binding ratio of the cell, and κ_B is the Ca^{2+}-binding ratio of exogenously added Ca^{2+} buffers with fast binding kinetics, such as the Ca^{2+} indicator. The calyx of Held has an endogenous Ca^{2+}-binding ratio, κ_S, of $\sim$40 (Helmchen et al., 1997). In the limit of [Ca^{2+}]$_i$ $\ll$ K_d, κ_B can be obtained with $\kappa_B = $ [fura-6F]/K_d, and thus, κ_B is 100/15 $\sim$ 7 under our conditions. Thus, the Ca^{2+}-binding capacity added exogenously by 80–100 μM fura-6F is small compared with the endogenous (fixed) Ca^{2+} buffer capacity of the calyx. Hence, 100 μM fura-6F should be well suited to faithfully measure the kinetics and the amplitude of [Ca^{2+}]$_i$ in the calyx of Held.

Model calculations. We calculated the time course of [Ca^{2+}]$_i$ according to a one-compartment model of cellular Ca^{2+} binding and extrusion in the presence and absence of parvalbumin (see Fig. 7). The model assumed that intracellular free Ca^{2+} is instantaneously bound to an endogenous buffer with a buffer capacity κ_S and more slowly bound to parvalbumin and/or extruded from the compartment with rate constant γ. Parvalbumin is either free, Ca^{2+} bound, or Mg^{2+} bound. The resulting differential equations (Lee et al., 2000) were solved numerically by fourth-order Runge–Kutta integration, using the following parameters for divalent binding of parvalbumin: $k_{off,Mg}$, 25 s^{-1}; $K_{d, Mg}$, 31 μM; $k_{off,Ca}$, 1 s^{-1}; $K_{d,Ca}$, 10 nM (Lee et al., 2000). The simulations in Figure 7 were calculated with 100 μM of the slow buffer, which corresponds to 50 μM parvalbumin, because parvalbumin has two functional Ca^{2+}-binding sites (Eberhard and Erne, 1994). The total Ca^{2+} load at the time of stimulation was 16 μM, and the baseline [Ca^{2+}]$_i$ was 50 nM. κ_S and γ were 40 and 500 s^{-1}, respectively, similar to previous estimates for the calyx of Held (Helmchen et al., 1997).

Data analysis. Data were analyzed using IgorPro (version 4.1; Wave-Metrics, Lake Oswego, OR) and is reported as mean $\pm$ SEM, and as mean $\pm$ SD in bar graphs. Paired or unpaired Student's t tests, as appropriate, were used to assess statistical significance (*$p < 0.05$; **$p < 0.01$; ***$p < 0.005$)

Results

[Ca^{2+}]$_i$ transients decay within tens of milliseconds in the unperturbed calyx of Held

To investigate how mobile Ca^{2+} buffers influence Ca^{2+} signaling in the calyx of Held, we studied the effect of whole-cell patch-clamp recording on spatially averaged [Ca^{2+}]$_i$ transients evoked by single APs and by brief high-frequency trains of APs. Whole-cell recording should lead to the diffusional loss of mobile Ca^{2+} buffers into the patch pipette. If calyces of Held contain a significant amount of mobile endogenous buffer with fast binding kinetics, we expect that whole-cell recording should lead to an increase in the amplitude and to an acceleration of the decay kinetics of [Ca^{2+}]$_i$, opposite to the effects observed during "overloading" cells with the fast Ca^{2+} buffer, fura-2 (Neher and Augustine, 1992; Helmchen et al., 1997). In contrast, whole-cell "wash-out" of a Ca^{2+} buffer with slow binding kinetics should prolong the decay of the [Ca^{2+}]$_i$ transient but leave its amplitude mostly unaffected (Atluri and Regehr, 1996; Lee et al., 2000) (see Fig. 7).

To assess the influence of whole-cell recordings on the [Ca^{2+}]$_i$ transient, we need to measure presynaptic [Ca^{2+}]$_i$ under conditions in which perturbation by a whole-cell recording pipette is minimized. For this purpose, we first "preloaded" a calyx of Held during a brief ($\sim$30 s) whole-cell recording episode with $\sim$80–100 μM of the Ca^{2+}-indicator fura-6F (Fig. 1A). Because of its relatively low-Ca^{2+} affinity (K_d, 15 μM; see Material and Methods), fura-6F should only minimally increase the endogenous Ca^{2+}-buffering ratio of the calyx and therefore allow us to faithfully measure the kinetics of [Ca^{2+}]$_i$. At the same time, the short duration of the whole-cell recording ($\sim$30 s) used for preloading the indicator dye should essentially preserve the endogenous mobile Ca^{2+} buffer.

After preloading with fura-6F and withdrawal of the pipette, we measured the [Ca^{2+}]$_i$ transient in response to single afferent fiber stimuli and to brief 100 Hz trains (Fig. 1C1,C2). In the example of Figure 1C1, the single AP-evoked [Ca^{2+}]$_i$ transient had an amplitude of 0.36 μM, and its decay was fitted with a double-exponential function, with fast and slow time constants of 33 and 385 ms, respectively. On average, the amplitude of the single AP-evoked [Ca^{2+}]$_i$ transient was 0.408 $\pm$ 0.05 μM ($n = 5$) (Fig. 1E), in good agreement with a previous estimate (Helmchen et al., 1997). However, the fast time constant of [Ca^{2+}]$_i$ decay was approximately threefold faster ($\tau_{fast} = 25 \pm 7$ ms; $n = 5$) (Fig. 1C,E, left) than the time constant of $\sim$80–100 ms estimated previously (Helmchen et al., 1997).

After measuring the [Ca^{2+}]$_i$ transients in a calyx briefly preloaded with fura-6F, we patched the same terminal again, using a patch pipette containing 100 μM fura-6F. This allowed us to compare the [Ca^{2+}]$_i$ transients during continuous whole-cell recording and under conditions of brief preloading. As shown in Figure 1D1, the decay of [Ca^{2+}]$_i$ in response to single APs was slower during continuous whole-cell recording. By pair-wise comparison within each cell (pre-load vs re-patch), we found a highly significant slowing of the fast time constant of the [Ca^{2+}]$_i$ decay, from 25 $\pm$ 7 ms after brief preloading to 80 $\pm$ 6 ms during continuous whole-cell recordings after repatching (Fig. 1E) ($n = 5$ cells; $p = 0.009$). The slow time constant of the [Ca^{2+}]$_i$ decay was not significantly changed after repatching (650 $\pm$ 84 ms; $n = 5$; $p = 0.28$). The amplitude of the [Ca^{2+}]$_i$ transient was slightly increased (preloading, 0.408 $\pm$ 0.05 μM; repatching, 0.5 $\pm$ 0.07 μM; $p = 0.048$) (Fig. 1E, right), but the relative amplitude effect ($\sim$1.2-fold) was small compared with the approximately three-

fold slowing of the fast component (τ_{fast}) of the [Ca^{2+}]$_i$ decay. The slowing of the [Ca^{2+}]$_i$ transient observed during continuous whole-cell recording might indicate the loss of a mobile endogenous Ca^{2+} buffer with slow Ca^{2+}-binding rate, which normally speeds up the decay of [Ca^{2+}]$_i$.

We also measured the [Ca^{2+}]$_i$ signal in response to brief 100 Hz trains of 10 APs (Fig. 1$C2,D2$). The build-up of [Ca^{2+}]$_i$ at the end of the 100 Hz trains was higher under whole-cell recording compared with the preloading condition (2.94 ± 0.3 and 2.2 ± 0.2 μM [Ca^{2+}]$_i$, respectively; $p = 0.032$) (Fig. 1F, right panel). This is probably caused by the faster decay of [Ca^{2+}]$_i$ after each AP under unperturbed conditions (Fig. 1$C1$), which will limit the cumulative build-up of [Ca^{2+}]$_i$ during repetitive stimulation. The decay of [Ca^{2+}]$_i$ after the 100 Hz train was also slower during whole-cell recordings compared with the preloading condition (Fig. 1F, left panel) ($p = 0.01$), similarly as observed after single stimuli.

The rapid decay of [Ca^{2+}]$_i$ is restored by the slow Ca^{2+} buffers EGTA or parvalbumin

We hypothesize that the slowing of the [Ca^{2+}]$_i$ decay under prolonged whole-cell recording (Fig. 1) is caused by presynaptic whole-cell dialysis of a Ca^{2+} buffer with slow binding kinetics. In this case, adding exogenous Ca^{2+} buffers with similar properties should restore the fast decay of [Ca^{2+}]$_i$. To test this, we made presynaptic whole-cell recordings with 100 μM fura-6F to measure [Ca^{2+}]$_i$ and added various exogenous Ca^{2+} buffers (Fig. 2A–C). With 100 μM fura-6F alone, the decay of the single AP-induced [Ca^{2+}]$_i$ transient was slow (Fig. 2A), with an average fast decay time constant of 105 ± 19 ms ($n = 4$) (Fig. 2E, open bar), confirming the results shown in Figure 1. In the additional presence of 100 μM EGTA, the fast decay time constant of [Ca^{2+}]$_i$ was 17 ms in the example of Figure 2B, and the average value was 21 ± 6 ms ($n = 4$) (Fig. 2E, gray bar), significantly faster than in the absence of EGTA ($p = 0.002$). However, the amplitude of [Ca^{2+}]$_i$ was unchanged (Fig. 2F) (control, 0.45 ± 0.14 μM; EGTA, 0.41 ± 0.04 μM; $p = 0.7$). Thus, 100 μM EGTA in the presynaptic pipette solution restored the fast kinetics of the [Ca^{2+}]$_i$ decay.

A good candidate for a mobile endogenous Ca^{2+} buffer is the Ca^{2+}-binding protein parvalbumin, which is present in calyces of Held from approximately P6 onward (Lohmann and Friauf, 1996; Felmy and Schneggenburger, 2004). Parvalbumin has a slow Ca^{2+}-binding rate (Lee et al., 2000) and a high diffusional
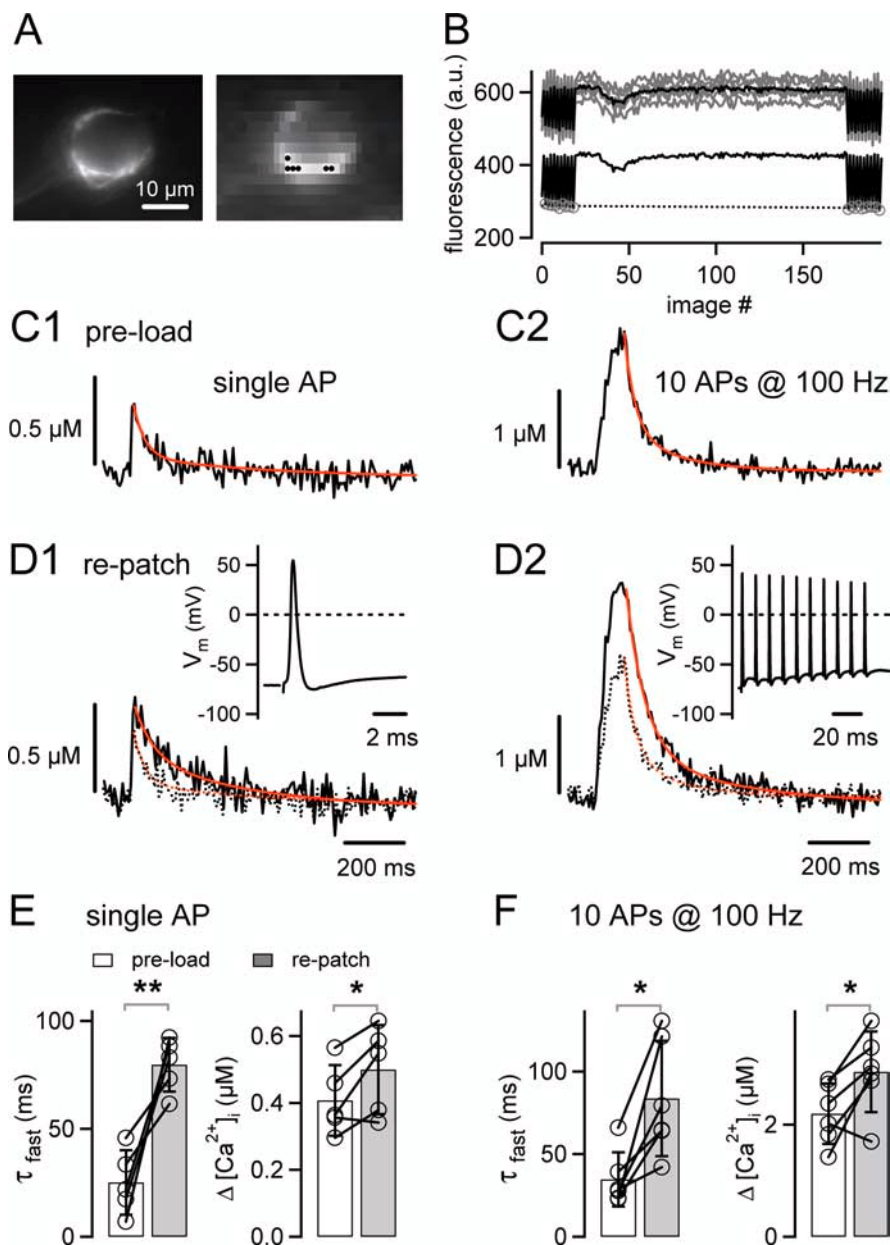

Figure 1. Rapid decay of AP-induced [Ca^{2+}]$_i$ transients in unperturbed calyces of Held. **A**, Fluorescence image showing a calyx of Held that was preloaded with 80 –100 μM fura-6F during a brief (~30 s) whole-cell recording (left image taken at 1 × 1 pixel binning; right image taken at 8 × 15 binning). Scale bar, 10 μm. **B**, Fluorescence signals (top gray traces) of the six superpixels marked in **A** (black dots in right image) and the resulting average fluorescence signal (superimposed black trace) during a single 100 Hz train of 10 stimuli. The bottom black trace represents the background-corrected average fluorescence signal. The F_{355} values (gray circles) measured before and after the stimulation were linearly interpolated (black dotted line) and used to calculate the fluorescence ratio (see Materials and Methods). **C**, Average [Ca^{2+}]$_i$ transients elicited by single APs (average of $n = 32$ traces; **C1**) or by 10 APs at 100 Hz (average of $n = 4$; **C2**) in a calyx preloaded with fura-6F. The decays of both [Ca^{2+}]$_i$ transients were fitted with double exponentials (red traces). **D**, Average [Ca^{2+}]$_i$ transients evoked by single APs (**D1**) and by 10 APs at 100 Hz (**D2**), as assessed during a continuous whole-cell recording with 100 μM fura-6F of the same terminal as shown in **A–C**. For comparison, the corresponding [Ca^{2+}]$_i$ transients obtained after preloading (**C**) are shown as dotted traces. The insets depict presynaptic APs measured in response to single stimuli and 100 Hz trains. Data in **A–D** are from the same cell. **E**, Fast decay time constants (τ_{fast}; left) and mean amplitudes (right) of single AP-evoked [Ca^{2+}]$_i$ transients recorded in $n = 5$ rat calyces after preloading (open bar) and after repatching (gray bar). Note the significant slowing after repatching ($p = 0.009$). **F**, Fast decay time constants (τ_{fast}; left) and amplitudes ([Ca^{2+}]$_i$; right) of [Ca^{2+}]$_i$ transients in response to the 100 Hz trains.

mobility (Schmidt et al., 2003a). Therefore, we next aimed to restore the fast decay of [Ca^{2+}]$_i$ by adding recombinant parvalbumin to the patch-pipette solution (see Materials and Methods). With 50 μM parvalbumin, the fast component of the [Ca^{2+}]$_i$ decay was accelerated to 64 ± 17 ms ($n = 3$ cells), but this
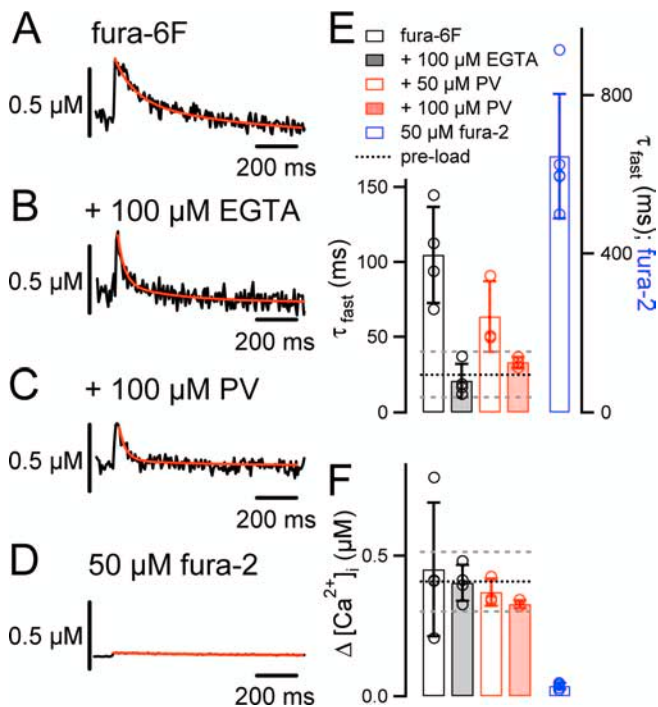
Figure 2. The slow Ca²⁺ buffers EGTA and parvalbumin restore the fast decay of AP-evoked [Ca²⁺]ᵢ transients. **A**, AP-evoked [Ca²⁺]ᵢ transient (average of n = 21 sweeps) during presynaptic whole-cell recording of a calyx of Held with 100 μM fura-6F in the pipette solution. **B**, A [Ca²⁺]ᵢ transient (average of n = 32) from another calyx, recorded with 100 μM fura-6F and 100 μM EGTA in the pipette solution. **C**, Example of a [Ca²⁺]ᵢ transient (average of n = 18) measured in a rat calyx with 100 μM fura-6F and 100 μM parvalbumin added to the presynaptic pipette solution. Note that the [Ca²⁺]ᵢ transients decay more rapidly in the presence of EGTA (**B**) and parvalbumin (**C**) compared with the no-added buffer condition (**A**). **D**, Example of a [Ca²⁺]ᵢ transient (average of n = 10 sweeps) recorded with 50 μM fura-2. Note the small amplitude and the slow decay of [Ca²⁺]ᵢ. In **A–D**, red lines are double-exponential (**A–C**) or single-exponential (**D**) fits of the [Ca²⁺]ᵢ decay. **E**, Average fast decay time constants (τ_fast) of AP-evoked [Ca²⁺]ᵢ transients of calyces of Held recorded with 100 μM fura-6F (open bars; n = 4 cells), 100 μM fura-6F and 100 μM EGTA (gray bars; n = 4 cells), 100 μM fura-6F and 50 μM parvalbumin (open red bar; n = 3 cells), 100 μM fura-6F and 100 μM parvalbumin (filled red bar; n = 4), or 50 μM fura-2 (blue bar; n = 5). The fura-2 data, which have an order of magnitude slower [Ca²⁺]ᵢ decay, are plotted on the right y-axis. Note that 100 μM parvalbumin restored the rapid [Ca²⁺]ᵢ decay observed in unperturbed calyces of Held (Fig. 1 E) (p = 0.4). **F**, Mean [Ca²⁺]ᵢ amplitudes measured under the various Ca²⁺ buffer conditions. The black and gray dotted lines in **E** and **F** represent the average ± SD of the corresponding values obtained in measurements of unperturbed calyces of Held (Fig. 1 E).

effect did not reach statistical significance with respect to the condition with fura-6F alone (Fig. 2 E, compare open bar and open red bar) (p = 0.12). In the next series of experiments, we therefore increased the parvalbumin concentration to 100 μM (Fig. 2 C), which significantly accelerated the decay of [Ca²⁺]ᵢ (τ_fast = 36 ± 4 ms; n = 4; p = 0.006) (Fig. 2 E, red bar) with respect to the condition of fura-6F alone (Fig. 2 A). This value of τ_fast was not significantly different from the one observed in the nonperturbed calyces of Held (Fig. 1 E) (τ_fast = 25 ± 7 ms; p = 0.21). Thus, parvalbumin restored the rapid decay of [Ca²⁺]ᵢ in a concentration-dependent manner. At the same time, parvalbumin did not significantly alter the amplitude of the [Ca²⁺]ᵢ transient compared with the condition of fura-6F alone (Fig. 2 F, compare open black bar and red bar) (p = 0.42). These findings are compatible with the idea that the slowing of the [Ca²⁺]ᵢ transient during whole-cell recording (Fig. 1 E) is caused by the diffusional loss of parvalbumin from calyces of Held.

To investigate whether a low concentration of an endogenous mobile Ca²⁺ buffer with fast Ca²⁺-binding kinetics is present in

calyces of Held, we repeated the presynaptic whole-cell recordings with 50 μM fura-2, a fast BAPTA-like Ca²⁺ buffer with a high Ca²⁺ affinity (K_d, 0.2 μM). Under this condition, the amplitude of the [Ca²⁺]ᵢ transient was strongly reduced (to 0.036 ± 0.011 μM), and the decay time constant of [Ca²⁺]ᵢ was prolonged (τ = 679 ± 150 ms) (Fig. 2 D–F). This is expected, because adding a high-affinity Ca²⁺ buffer with fast Ca²⁺-binding kinetics to a cell with low endogenous Ca²⁺-buffering capacity, κ_s, strongly influences the amplitude and the decay kinetics of [Ca²⁺]ᵢ (Neher and Augustine, 1992; Helmchen et al., 1997). This demonstrates that the effects of whole-cell recording on the [Ca²⁺]ᵢ transient (approximately threefold slowing of the fast decay time constant) (Fig. 1) cannot be explained by assuming a wash-out of a significant concentration (10 μM or more) of a high-affinity mobile Ca²⁺ buffer with fast binding kinetics (see Discussion).

The decay of paired-pulse facilitation is determined by a mobile endogenous Ca²⁺ buffer

We next studied the role of mobile endogenous Ca²⁺ buffer(s) in short-term facilitation of transmitter release at the calyx of Held. We first measured paired-pulse facilitation under conditions in which the nerve terminal is unperturbed by using fiber stimulation in the absence of presynaptic whole-cell recordings (Fig. 3).

To isolate facilitation at this depressing synapse, we lowered the extracellular Ca²⁺ concentration ([Ca²⁺]ₑ) to 0.6 mM. This led to a decrease of the first EPSC amplitude and reversed paired-pulse depression (data not shown) to paired-pulse facilitation. Facilitation was probed by pairs of stimuli and analyzed once the EPSC amplitudes attained a stable value after lowering [Ca²⁺]ₑ (Fig. 3A, black bar) (final EPSC amplitude, 1.14 ± 0.08 nA; n = 6 cells). Paired-pulse facilitation was maximal at the shortest interstimulus interval of 4 ms (Fig. 3B) (206 ± 12%; n = 6 cells) (Fig. 3E) and then decayed, giving way to a small but consistently observed paired-pulse depression at an interstimulus interval of 400 ms (Fig. 3B,C) (88 ± 5% of the control EPSC; p = 0.058; one-sample t test). The decay of facilitation could be fitted with a single-exponential function, with a time constant of 33 ms for the cell shown in Figure 3C. On average, paired-pulse facilitation decayed with a time constant (τ) of 35 ± 5 ms (Fig. 3D) (n = 6 cells). This value is surprisingly fast when compared with the decay of facilitation at other CNS synapses (Mennerick and Zorumski, 1995; Atluri and Regehr, 1996), but it matches the fast decay time constant of presynaptic [Ca²⁺]ᵢ measured in unperturbed conditions at the calyx of Held (τ_Ca, fast, 25 ± 7 ms) (Fig. 1 E).

The decay of paired-pulse facilitation is probably determined by the duration of the spatially averaged [Ca²⁺]ᵢ transient in the nerve terminal (Atluri and Regehr, 1996; Felmy et al., 2003). Because the [Ca²⁺]ᵢ transient was slowed during presynaptic whole-cell recordings (Fig. 1), the decay of paired-pulse facilitation should also be slowed under presynaptic whole-cell recording conditions. To test this, we made paired presynaptic and postsynaptic whole-cell voltage-clamp recordings and studied the time course of paired-pulse facilitation (Fig. 4). Brief pairs of identical voltage-clamp steps from −80 to +28 mV were applied presynaptically, and the durations of these steps (0.6–1.2 ms) were adjusted such that the resulting first EPSC amplitudes (1.39 ± 0.09 nA; n = 22 cell pairs) were comparable with the ones obtained during afferent fiber stimulation (p = 0.2) (Fig. 1).

In Figure 4A, the results from a recording without presynaptically added Ca²⁺ buffer are shown. A paired-pulse facilitation of ~200% was observed, which decayed slowly (time constant, 93 ms) (Fig. 4A2). On average, facilitation in the absence of added

Ca²⁺ buffer decayed with a time constant of 85 ± 15 ms ($n = 5$ cells) (Fig. 4F, open bar) and, thus, significantly slower than during afferent fiber stimulation ($p = 0.009$) (Fig. 3). When we added EGTA to the presynaptic pipette solution (Fig. 4B), facilitation decayed with an average time constant of 27 ± 2 ms ($n = 2$ cells with 100 μM EGTA, and $n = 2$ cells with 75 μM EGTA) (Fig. 4F, gray bar), significantly faster than in the absence of added Ca²⁺ buffer ($p = 0.012$) (Fig. 4F, open bar). In contrast, neither the amplitude of paired-pulse facilitation ($222 \pm 33\%$) (Fig. 4H, gray bar) nor the initial EPSC amplitude (1.17 ± 0.26 nA; $n = 4$ cells) were significantly different from their control values obtained in the absence of EGTA ($p = 0.43$ and 0.58, respectively). Thus, adding 75 or 100 μM EGTA to the presynaptic terminal rescues the fast decay of paired-pulse facilitation observed under conditions of afferent fiber stimulation (Fig. 3).

In these presynaptic and postsynaptic voltage-clamp recordings of paired-pulse facilitation, we also observed that the presynaptic Ca²⁺ current slightly facilitated (to $108 \pm 0.4\%$ of control; $n = 4$) at the shortest interval of 4 ms (Fig. 4A1, top panel). This Ca²⁺-current facilitation (Borst and Sakmann, 1998; Cuttle et al., 1998; Tsujimoto et al., 2002) gave way to a slight Ca²⁺-current depression at the longest interval studied (400 ms; to $90.5 \pm 0.9\%$ of control) (Xu and Wu, 2005). Based on the supralinear relationship between Ca²⁺ influx and transmitter release, with a power function with exponent of ~3.5 (Schneggenburger et al., 1999; Xu and Wu, 2005), we estimate that Ca²⁺-current facilitation causes a facilitation of transmitter release to ~135% of control, corresponding to approximately one-fourth of the overall facilitation of transmitter release. The exact contribution of Ca²⁺-current facilitation should be determined in future work.

The results in Figure 4, A and B, show that 75–100 μM EGTA restores the fast kinetics of paired-pulse facilitation observed under conditions of afferent fiber stimulation (Fig. 3). We expect that the accelerated decay of paired-pulse facilitation was caused by a speeding of the [Ca²⁺]ᵢ transient in the presence of EGTA (Fig. 2B). To verify this directly, we made paired recordings with 100 μM fura-6F in the presynaptic pipette solution to measure the [Ca²⁺]ᵢ transient caused by single presynaptic voltage-clamp pulses. This was done both with fura-6F alone (Fig. 4C) as well as with fura-6F and 75 μM EGTA (Fig. 4D). With fura-6F alone, the [Ca²⁺]ᵢ transient and paired-pulse facilitation decayed quite slowly ($\tau_{fast, Ca}$, 95 ± 17 ms; $\tau_{facilitation}$, 69 ± 13 ms) (Fig. 4F,G, open red bars). With fura-6F and 75 μM EGTA, the decay of both [Ca²⁺]ᵢ and paired-pulse facilitation were accelerated ($\tau_{fast, Ca}$, 25 ± 6 ms; $\tau_{facilitation}$, 28 ± 6 ms) (Fig. 4F,G, red bars). Thus, EGTA restores the fast decay of paired-pulse facilitation by speeding up the decay of the presynaptic [Ca²⁺]ᵢ transient.

In an additional test of Ca²⁺ buffers added to the presynaptic pipette solution, we used 50 μM fura-2 and measured the presynaptic [Ca²⁺]ᵢ transient and paired-pulse facilitation in the pres-
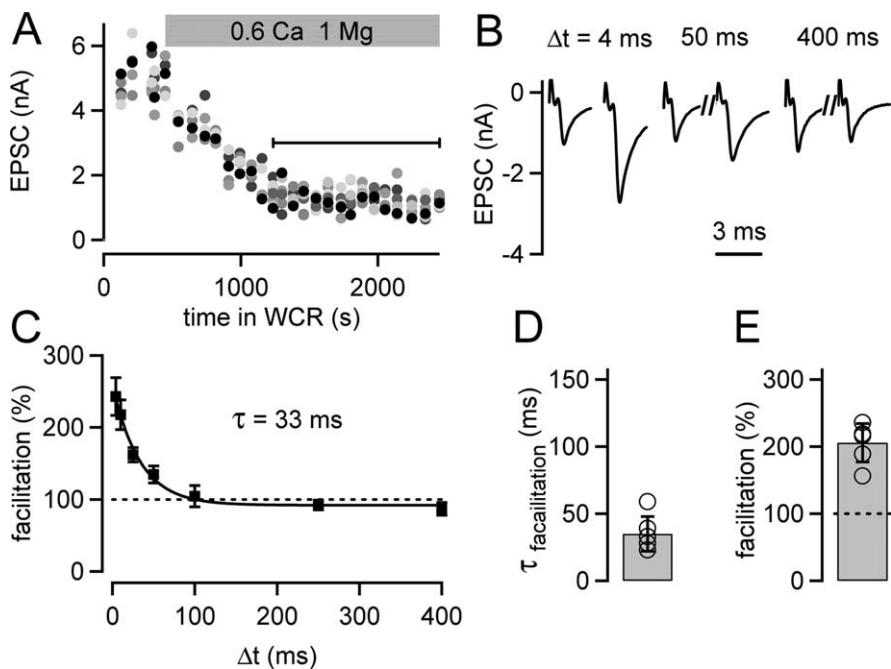
Figure 3. Paired-pulse facilitation under conditions of afferent fiber stimulation decays surprisingly fast at the calyx of Held. **A**, EPSC amplitudes in response to the first stimulus of pairs of afferent fiber stimuli, plotted as a function of time in whole-cell recording (WCR). Paired pulses were applied at various intervals. The first EPSC amplitude for each interstimulus interval is shown, and the grayscale code identifies the length of the interstimulus interval (black symbol, 4 ms; longer intervals are represented by increasingly lighter gray tones). At the time indicated by the gray bar, the extracellular [Ca²⁺] was changed from 2 to 0.6 mM. The analysis of paired-pulse facilitation was restricted to the phase of the experiment during which the effect of the low extracellular [Ca²⁺] had stabilized (black line). **B**, Average EPSCs ($n = 15$ sweeps) in response to pulse pairs given at three different interstimulus intervals (Δt) that were recorded during the period specified by the black line in **A**. **C**, Paired-pulse facilitation (facilitation = average EPSC2/average EPSC1 × 100) as a function of Δt of the cell shown in **A** and **B**. The average data points ($n = 15$ repetitions) were fitted by an exponential function yielding a time constant (τ) of 33 ms. **D**, Mean decay time constants of facilitation of $n = 6$ individual cells (open circles). **E**, The average maximal facilitation ($n = 6$ cells) measured at the shortest interstimulus interval of 4 ms.

ence of this fast, BAPTA-like Ca²⁺ buffer (Fig. 4E). In the presence of fura-2, the [Ca²⁺]ᵢ transient was strongly suppressed and prolonged (Fig. 4E, bottom panel, G, blue bar), confirming the results obtained in Figure 2D with 50 μM fura-2. The amplitude of paired-pulse facilitation was $162 \pm 15\%$ ($n = 4$), smaller than facilitation measured under conditions of afferent fiber stimulation (Fig. 3) ($p = 0.043$). Also, with 50 μM fura-2, facilitation decayed very fast, with a mean time constant of only 18 ± 5 ms (Fig. 4F). This might indicate a suppression of facilitation for times longer than 10 ms, probably caused by the strong reduction of the free [Ca²⁺]ᵢ transient exerted by this fast Ca²⁺ buffer. The effects of 50 μM fura-2 on the [Ca²⁺]ᵢ transient and on facilitation make it unlikely that calyces of Held contain a sizable amount of a mobile Ca²⁺ buffer with fast binding kinetics. However, it remains possible that calyces contain immobile Ca²⁺ buffer(s) with fast-binding kinetics. Also, mobile fast Ca²⁺ buffer(s), like calretinin, might be expressed at later developmental stages (Felmy and Schneggenburger, 2004) (see Discussion).

Summarizing the experiments with exogenously added buffers shown in Figure 4, it is seen that with 75–100 μM EGTA, both facilitation and the [Ca²⁺]ᵢ transient decay with a (fast) time constant of ~30 ms (Fig. 4F,G, arrowheads), similarly, as observed in the unperturbed conditions (Figs. 1, 3). Also, the amplitude of paired-pulse facilitation observed with 75–100 μM EGTA (~220%) (Fig. 4H, arrowheads) is comparable with the one observed with afferent fiber stimulation (Fig. 3). Because low concentrations of EGTA restore both the decay of [Ca²⁺]ᵢ and

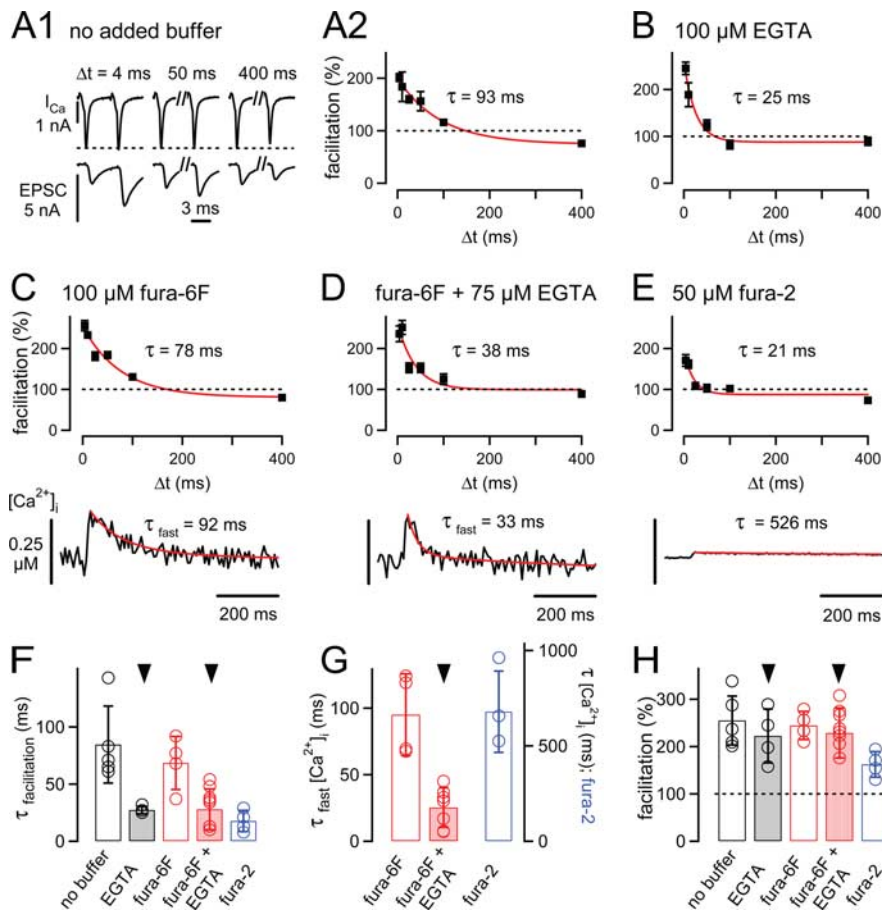**Figure 4.** The influence of presynaptically added Ca²⁺ buffers on paired-pulse facilitation and presynaptic [Ca²⁺]ᵢ transients. **A1**, Examples of presynaptic whole-cell calcium currents (I_{Ca}) and EPSCs in response to paired voltage-clamp pulses of three different interstimulus intervals (Δt). **A2**, Paired-pulse facilitation (mean ± SEM) of the recording shown in **A1**. The data were fitted with an exponential function, with time constant τ = 93 ms. **B**, Paired-pulse facilitation in another cell pair, in which 100 μM EGTA was added to the presynaptic intracellular solution. Note the accelerated decay of facilitation. **C**, Mean facilitation (top) and presynaptic [Ca²⁺]ᵢ (bottom) measured with 100 μM fura-6F added to the presynaptic pipette solution. **D**, Facilitation and presynaptic [Ca²⁺]ᵢ transient in a cell pair recorded with 100 μM fura-6F and 75 μM EGTA in the presynaptic pipette solution. **E**, Facilitation and presynaptic [Ca²⁺]ᵢ of a cell pair recorded with 50 μM fura-2 in the presynaptic pipette solution. In **A2–E**, red lines are single- or double-exponential fits, with the time constants (τ) or fast time constants in the case of double-exponential fits (τ_fast) as indicated. **F**, Average decay time constants of facilitation recorded under the various conditions of presynaptically added Ca²⁺ buffer. Note the significant speeding of the decay of facilitation to ∼30 ms induced by 100 μM EGTA (p = 0.029) or by 75 μM EGTA and 100 μM fura-6F (p = 0.005). **G**, Average fast decay time constants of [Ca²⁺]ᵢ transients recorded with 100 μM fura-6F without added buffer (red open bar; n = 4 cells) and with 75 μM EGTA (n = 9; red bar). The blue bar (right ordinate) shows the average decay time constant of [Ca²⁺]ᵢ (monoexponential fit) measured with 50 μM fura-2 (n = 3). EGTA (75 μM) significantly (p = 0.0005) accelerated the decay of [Ca²⁺]ᵢ compared with the no-added buffer condition (arrowhead). **H**, Amplitude of facilitation under the different conditions of presynaptically added Ca²⁺ buffers. Note the significant decrease in facilitation in the presynaptic presence of 50 μM fura-2 (blue bar).

the decay of facilitation observed under unperturbed conditions (Figs. 1, 3), it is likely that an endogenous Ca²⁺ buffer with slow binding kinetics normally accelerates the decay of [Ca²⁺]ᵢ, and that whole-cell recording leads to the wash-out of this slow endogenous Ca²⁺ buffer.

The decay of presynaptic [Ca²⁺]ᵢ and facilitation is slowed in parvalbumin knock-out mice

To investigate whether parvalbumin represents the mobile presynaptic Ca²⁺ buffer with slow Ca²⁺-binding kinetics that is lost during presynaptic whole-cell recordings (Figs. 1–4), we investigated parvalbumin knock-out mice (PV−/−) (Schwaller et al., 1999). Considering the results obtained thus far, we expect that

calyces of PV−/− mice show a prolonged decay of [Ca²⁺]ᵢ and paired-pulse facilitation.

We first measured the [Ca²⁺]ᵢ transient evoked by single APs with the preloading method of fura-6F (Fig. 1), both in calyces of PV−/− mice (Fig. 5A) as well as in wild-type control mice (Fig. 5B). The decay of the [Ca²⁺]ᵢ transient was significantly slower in PV−/− mice (τ_fast, 70 ± 7 ms; n = 11) (Fig. 5A,C) compared with wild-type mice (τ_fast, 31 ± 5 ms; n = 7; p = 0.0005) (Fig. 5B,C). In contrast, the amplitudes of the [Ca²⁺]ᵢ transients were not significantly different (PV−/−, 0.35 ± 0.08 μM; wild-type, 0.43 ± 0.07 μM; p = 0.42) (Fig. 5D). The [Ca²⁺]ᵢ decay in wild-type mice (τ_fast, ∼31 ms) was in excellent agreement with the decay of [Ca²⁺]ᵢ measured with the same approach in rat calyces of Held (brief preloading) (Fig. 1C,E). The similar decay kinetics of [Ca²⁺]ᵢ between the two species indicates that parvalbumin is present presynaptically in both rats and mice. Immunohistochemistry also demonstrated that parvalbumin is present in calyces of Held in both species (Felmy and Schneggenburger, 2004).

Finally, we measured the kinetics of paired-pulse facilitation in PV−/− mice (Fig. 6). We used afferent fiber stimulation under conditions of low extracellular Ca²⁺ (Fig. 3) to avoid wash-out of the presynaptic terminal. Representative EPSCs in response to three interstimulus intervals, which were recorded in a PV−/− cell, are shown in Figure 6A1. Facilitation decayed slowly, with a time constant of 77 ms in this cell (Fig. 6A2), and the average decay time constant of facilitation in PV−/− mice was 62 ± 11 ms (n = 8) (Fig. 6C). In wild-type mice (Fig. 6B), facilitation decayed significantly faster, with an average time constant of 31 ± 11 ms across cells (n = 7; p = 0.039) (Fig. 6C). In contrast, both the amplitude of facilitation (Fig. 6D) (PV−/−, 189.2 ± 9%; wild-type, 190.2 ± 25%; p = 0.97) and the first EPSC amplitudes (PV−/−, 1.31 ± 0.18 nA; wild-type, 1.31 ± 0.76 nA; p = 0.99) were similar between the two genotypes. Thus, in PV −/− mice, the decay of the [Ca²⁺]ᵢ transient (Fig. 5) and the decay of paired-pulse facilitation is slowed, whereas the amplitudes of [Ca²⁺]ᵢ and paired-pulse facilitation are unchanged. This closely mirrors the effects of presynaptic whole-cell recordings on [Ca²⁺]ᵢ transients and paired-pulse facilitation in rats (Figs. 1, 3, 4), indicating that parvalbumin is the main endogenous mobile Ca²⁺ buffer in young calyces of Held.

Modeling the impact of parvalbumin on the spatially averaged [Ca²⁺]ᵢ signal

To verify whether the surprisingly fast decay rate of the spatially averaged presynaptic [Ca²⁺]ᵢ transient observed under unper-
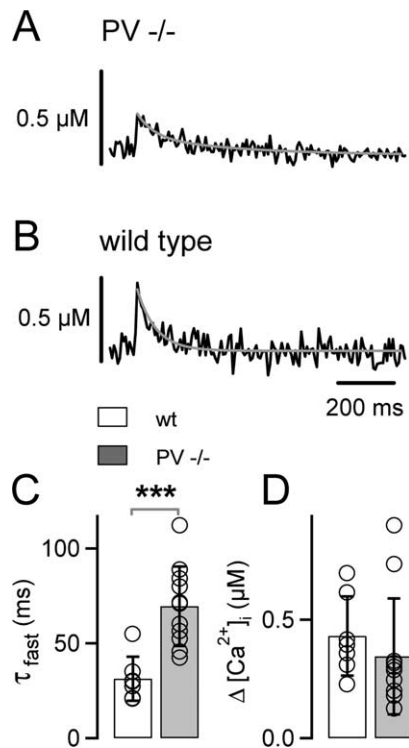
Figure 5. AP-induced presynaptic [Ca^{2+}]$_i$ transients decay slowly in parvalbumin knockout mice. **A, B,** Example of [Ca^{2+}]$_i$ transients in a calyx of Held from a PV−/− mouse (**A**) and from a wild-type (wt) mouse (**B**). The decay of the [Ca^{2+}]$_i$ transients were fitted with double-exponential functions (gray traces). **C, D,** Average fast decay time constants (τ_{fast}; **C**) and average amplitudes ([Ca^{2+}]$_i$; **D**) of [Ca^{2+}]$_i$ transients elicited by single APs in PV−/− (gray bars; $n = 11$ cells) and in wild-type (white bars; $n = 7$ cells). Note the significant slowing ($p = 0.0005$) of the [Ca^{2+}]$_i$ transients in PV−/− mice, whereas the [Ca^{2+}]$_i$ amplitudes were not significantly different ($p = 0.42$).

turbed conditions (τ_{fast}, ~30 ms) (Figs. 1, 5) is compatible with the kinetic properties of Ca^{2+} binding to parvalbumin (Lee et al., 2000), we simulated the spatially averaged [Ca^{2+}]$_i$ transient according to a modified one-compartment model of Ca^{2+} signaling, taking into account the presence of a Ca^{2+} buffer with slow binding kinetics (see Materials and Methods).

We first simulated the [Ca^{2+}]$_i$ transient in the absence of parvalbumin, assuming a low endogenous Ca^{2+} buffer capacity (κ_S) of 40 and a high Ca^{2+} extrusion rate γ of 500 s^{-1} [see Helmchen et al. (1997) and Materials and Methods for the remaining parameters]. The resulting simulated [Ca^{2+}]$_i$ transient had an amplitude of ~0.45 μM and decayed with a single-exponential time constant of 80 ms (Fig. 7, gray trace), similar to the experimentally observed [Ca^{2+}]$_i$ transients measured with fura-6F during prolonged whole-cell recordings (Figs. 1, 2, 4). Introducing 50 μM of the slow Ca^{2+} buffer parvalbumin increased the rate of decay of the simulated [Ca^{2+}]$_i$ transient, which was now best fitted by a double-exponential function with a fast time constant of 31 ms (Fig. 7, black trace). Thus, the fast decay rate of the [Ca^{2+}]$_i$ transients measured here under unperturbed conditions (τ_{fast}, ~30 ms) (Figs. 1, 5) are compatible with the action of a moderate concentration of a Ca^{2+} buffer with slow binding kinetics. Therefore, the combination of a low endogenous fixed Ca^{2+} buffer capacity (κ_S), a high cellular Ca^{2+}-extrusion rate, and a Ca^{2+}-binding protein with slow Ca^{2+}-binding kinetics produce a surprisingly fast decay of the spatially averaged [Ca^{2+}]$_i$ transients in these large nerve terminals. This mechanism might be shared by other nerve terminals in the au-

ditory pathway that also express parvalbumin (Pór et al., 2005) (see Discussion).

Discussion

Here, we functionally identify parvalbumin as an endogenous mobile Ca^{2+} buffer at the calyx of Held nerve terminals of young rats and mice. Presynaptic whole-cell recordings made without added Ca^{2+} buffer prolonged the decay of the [Ca^{2+}]$_i$ transient without a large effect on its amplitude, and the fast kinetics of the [Ca^{2+}]$_i$ transient was restored by adding the slow Ca^{2+} buffers, EGTA or parvalbumin, to the pipette solution. Similarly, the decay of paired-pulse facilitation and its underlying residual Ca^{2+} signal were slowed during presynaptic whole-cell recording, and these effects were again prevented by adding low concentrations of EGTA. The slowing of the decay of [Ca^{2+}]$_i$ and of paired-pulse facilitation by presynaptic whole-cell recordings was closely mirrored in knock-out mice lacking parvalbumin, a Ca^{2+}-binding protein with slow binding kinetics. We thus conclude that parvalbumin accelerates the decay of [Ca^{2+}]$_i$ and paired-pulse facilitation at these large, glutamatergic nerve terminals.

An endogenous Ca^{2+} buffer with slow binding kinetics at the calyx of Held

Loading cells with exogenous high-affinity Ca^{2+} buffers or Ca^{2+} indicators is well known to influence the amplitude and/or the decay kinetics of the spatially averaged [Ca^{2+}]$_i$ transient, depending on whether the introduced Ca^{2+} buffers have fast or slow Ca^{2+}-binding kinetics (Neher and Augustine, 1992; Atluri and Regehr, 1996; Helmchen et al., 1997; Lee et al., 2000). Therefore, removing endogenous mobile Ca^{2+} buffers from the cytosol by whole-cell dialysis is expected to have the corresponding opposite effects on the [Ca^{2+}]$_i$ transient (Zhou and Neher, 1993), a prediction we used here to probe for mobile Ca^{2+} buffers at the calyx of Held. Our finding that continuous whole-cell recording leads to an approximately threefold slowing of the decay of [Ca^{2+}]$_i$ is consistent with the idea that an endogenous Ca^{2+} buffer with slow Ca^{2+}-binding kinetics is lost by diffusion into the whole-cell patch pipette.

The slow Ca^{2+} buffer EGTA (75–100 μM), and recombinant parvalbumin, at a nominal concentration of 100 μM restored the decay kinetics of [Ca^{2+}]$_i$, whereas 50 μM parvalbumin only partially restored the fast decay kinetics (Fig. 2). Because parvalbumin contains two Ca^{2+}-binding sites (Haiech et al., 1979; Eberhard and Erne, 1994), one would expect that 50 μM parvalbumin should be as effective as 100 μM EGTA. The slight (approximately twofold) discrepancy between the expected and the observed efficiency of exogenously added parvalbumin is most likely attributable to technical reasons, such as a lower effective concentration of the recombinant protein at the tip of the patch pipette (see Materials and Methods). The model calculations also indicated that 50 μM parvalbumin (equivalent to 100 μM Ca^{2+}-binding sites) is sufficient to account for a fast decay of [Ca^{2+}]$_i$ (τ_{fast}, ~30 ms) (Fig. 7). Therefore, we estimate that young calyces of Held contain ~50 μM parvalbumin, a concentration that is somewhat lower than the one estimated for dendrites of Purkinje cells (80 μM) (Schmidt et al., 2003b) and for axons of cerebellar interneurons (~150 μM) (Collin et al., 2005).

The similarity of the effects exerted by presynaptic whole-cell recordings (Figs. 1–4) or by genetic deletion of parvalbumin (Figs. 5, 6) on the decay of [Ca^{2+}]$_i$ and paired-pulse facilitation identifies parvalbumin as the endogenous Ca^{2+} buffer that washes out during presynaptic whole-cell recordings. This is in good agreement with immunohistochemical data (Felmy and
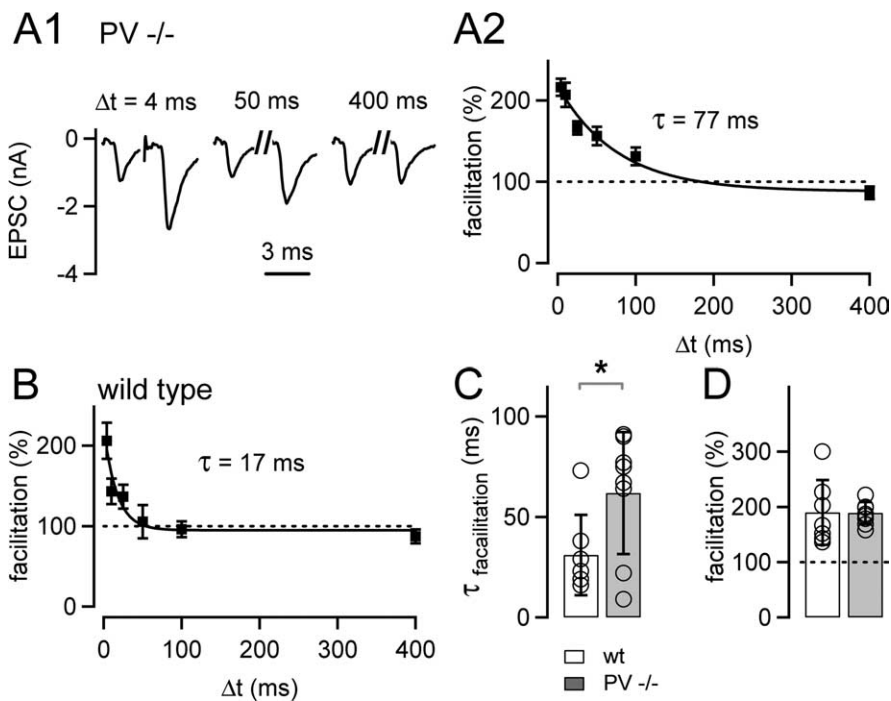
A1 PV -/-

B wild type

Figure 6. Paired-pulse facilitation decays slowly at the calyx of Held of parvalbumin knock-out mice. **A1**, Representative EPSCs in response to pulse pairs at three different interstimulus intervals (Δt) in a PV−/− cell, recorded at 0.6 mM extracellular [Ca²⁺]. **A2**, Mean facilitation as a function of the interstimulus interval of the PV−/− cell shown in **A1** ($n = 15$ repetitions). The data were fitted by an exponential function, with a time constant of 77 ms. **B**, Paired-pulse facilitation in a cell from a wild-type (wt) mouse ($n = 17$ repetitions). Note the fast decay of paired-pulse facilitation, with a time constant of 17 ms in this cell. **C**, Average decay time constants of paired-pulse facilitation obtained in $n = 8$ cells from PV−/− mice (gray bar), and in $n = 7$ cells from wild-type mice (white bar). Note the significantly ($p = 0.039$) slower decay of paired-pulse facilitation in PV−/− mice. **D**, The amplitude of paired-pulse facilitation was unchanged between wild-type mice (open bar; $n = 7$ cells) and PV−/− mice (gray bar; $n = 8$ cells; $p = 0.96$).
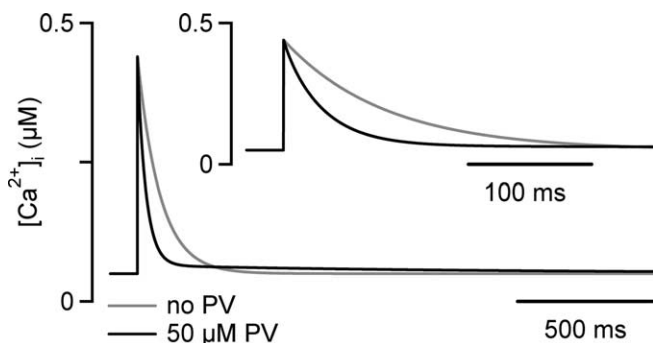

Figure 7. A modified single-compartment model of Ca²⁺ signaling at the calyx of Held. An AP-evoked, spatially averaged [Ca²⁺]ᵢ transient was simulated either in the absence of a slow Ca²⁺ buffer (gray trace) or in the presence of 50 μM parvalbumin (PV). See Materials and Methods for the parameters used in the simulation. The inset shows the simulated [Ca²⁺]ᵢ traces at increased time resolution. The simulated [Ca²⁺]ᵢ transient in the absence of parvalbumin (gray traces) was well fitted by a single-exponential function, with time constant $\tau = 78$ ms. In the presence of 50 μM parvalbumin, the initial decay of [Ca²⁺]ᵢ was accelerated, and the decay of [Ca²⁺]ᵢ was now best fit by a double-exponential function, with fast and slow time constants of 31 and 1310 ms, respectively. Note that the combination of a low endogenous Ca²⁺ buffer capacity ($\kappa_s = 40$), a fast Ca²⁺ extrusion rate ($\gamma = 500\ \text{s}^{-1}$), and the presence of a Ca²⁺ buffer with slow binding kinetics result in an extremely fast initial decay of spatially averaged [Ca²⁺]ᵢ.

Schneggenburger, 2004), which showed that calyces of Held express parvalbumin from approximately P6 onward, whereas Ca²⁺-binding proteins with fast binding kinetics are either absent from calyces of Held (calbindin D-28k) or only expressed at

a later developmental stage (calretinin). However, it is possible that Ca²⁺ buffering at the calyx of Held will be influenced by an additional fast Ca²⁺ buffer later in development, when a sizeable fraction of calyces become calretinin-positive from approximately P15 onward (Felmy and Schneggenburger, 2004).

The role of endogenous Ca²⁺ buffers in facilitation of transmitter release
A role for presynaptic parvalbumin in modulating short-term plasticity has been shown previously at inhibitory cerebellar synapses, where paired-pulse depression observed in wild-type mice changed to paired-pulse facilitation in PV−/− mice (Caillard et al., 2000). Parvalbumin acts as a slow Ca²⁺ buffer in axons of cerebellar interneurons, accelerating the decay of [Ca²⁺]ᵢ (Collin et al., 2005), but the exact role of parvalbumin in modulating paired-pulse facilitation has been less clear. Here, we show, by studying paired-pulse facilitation under conditions of minimized depression and by testing short interstimulus intervals, that parvalbumin speeds up the decay of facilitation twofold to threefold, causing a fast decay of paired-pulse facilitation of only ~30 ms at room temperature (Fig. 3). Thus, in addition to the ability of parvalbumin of converting paired-pulse facilitation into paired-pulse depression at inhibitory cerebellar (Caillard et al., 2000) and hippocampal (Vreugdenhil et al., 2003) synapses, we show that parvalbumin modulates the decay kinetics of paired-pulse facilitation at a large excitatory synapse, the calyx of Held.

The finding that an endogenous mobile Ca²⁺ buffer modulates the decay but not the amplitude of paired-pulse facilitation is unexpected in light of previous evidence for a "Ca²⁺ buffer saturation" mechanism of transmitter release facilitation. We previously observed that facilitation of transmitter release at the calyx could not be quantitatively accounted for by linear summation of the measured residual Ca²⁺ signal and the inferred local Ca²⁺ signal for transmitter release (Felmy et al., 2003), and we concluded that Ca²⁺ buffer saturation could cause a supralinearity in the summation of the two Ca²⁺ signals. At some hippocampal and cortical synapses, evidence for a Ca²⁺ buffer saturation mechanism involving the fast Ca²⁺-binding protein calbindin-D28k has also been obtained (Blatow et al., 2003; Jackson and Redman, 2003). A Ca²⁺ buffer that causes facilitation in the sense of the Ca²⁺ buffer saturation mechanism needs to have a fast Ca²⁺-binding rate to intercept with the local, near-membrane [Ca²⁺]ᵢ signal relevant for vesicle fusion (Neher, 1998; Matveev et al., 2004). Our present data show, however, that the main endogenous mobile Ca²⁺ buffer at calyces of Held of young rats and mice (P8–P10) is a slow Ca²⁺ buffer, which accelerates the decay of presynaptic [Ca²⁺]ᵢ and facilitation but does not modulate the amplitude of facilitation.

Recently, evidence against a global Ca²⁺ buffer saturation in calyces of Held of young rats has also been obtained by Habets and Borst (2006), who showed that [Ca²⁺]ᵢ transients during

high-frequency stimulation had constant amplitudes despite a strong build-up of residual Ca^{2+}, opposite of the expectations for Ca^{2+} buffer saturation. It remains possible that saturation of an immobile endogenous Ca^{2+} buffer contributes to transmitter release facilitation (Matveev et al., 2004), but in this case, one would have to assume that the immobile buffer does not significantly influence spatially averaged $[Ca^{2+}]_i$ transients, maybe because of a specific location close to the release sites. It should also be noted that the previous work (Felmy et al., 2003) [Habets and Borst, (2006), their Fig. 3] has been done under continuous whole-cell recording, likely causing wash-out of endogenous mobile Ca^{2+} buffers. Indeed, we observed that continuous whole-cell recordings led to a small increase in the amplitude of the spatially averaged $[Ca^{2+}]_i$ transient (~20%) (Fig. 1E), in addition to the strong effect on the decay kinetics of $[Ca^{2+}]_i$. This might indicate the wash-out of an endogenous Ca^{2+} buffer with fast binding kinetics and with a Ca^{2+}-binding capacity κ of ~10, which would correspond to ~5–10 μM high-affinity Ca^{2+} buffer with fast binding kinetics. Thus, we cannot exclude at present that a small fraction of the mobile Ca^{2+} buffers in the calyces of Held is represented by a fast buffer, but the main effect of whole-cell dialysis, a twofold to threefold slowing of the $[Ca^{2+}]_i$ transient and of paired-pulse facilitation, indicates the action of a mobile Ca^{2+} buffer with slow binding kinetics, primarily represented by parvalbumin.

When comparing different synapses, it becomes apparent that Ca^{2+}-binding proteins can differentially influence facilitation of transmitter release. The slow Ca^{2+} buffer parvalbumin speeds up the decay of paired-pulse facilitation at the calyx of Held (our study) and probably acts in a similar way at inhibitory synapses (Caillard et al., 2000), whereas calbindin D-28k acts as a fast, saturable Ca^{2+} buffer at mossy-fiber terminals and in specific inhibitory cortical interneurons, causing transmitter release facilitation by a buffer saturation mechanism (Blatow et al., 2003). In calyces of Held, the presence of a presynaptic Ca^{2+} buffer with slow binding kinetics, together with a low endogenous Ca^{2+} buffer capacity and a high Ca^{2+} extrusion rate (Helmchen et al., 1997) causes a surprisingly fast decay of the spatially averaged presynaptic $[Ca^{2+}]_i$ transient (Fig. 7), and this will limit the build-up of residual Ca^{2+} during high-frequency trains of APs. Interestingly, auditory brainstem neurons, many of which express parvalbumin (Celio, 1990; Lohmann and Friauf, 1996; Pór et al., 2005), as well as parvalbumin-containing cortical and cerebellar interneurons, can fire repetitively at high rates, probably enabled by fast-activating K^+ channels of the Kv3 subunit family, which are expressed quite specifically in these neuronal populations (Du et al., 1996; Martina et al., 1998; Wang et al., 1998; Macica et al., 2003) (for review, see Rudy and McBain, 2001). The expression of parvalbumin could thus serve as one adaptive mechanism that allows these fast-spiking neurons a more effective Ca^{2+} handling during high-frequency trains of APs.

References

Airaksinen MS, Eilers J, Garaschuk O, Thoenen H, Konnerth A, Meyer M (1997) Ataxia and altered dendritic calcium signaling in mice carrying a targeted null mutation of the calbindin D28k gene. Proc Natl Acad Sci USA 94:1488–1493.

Atluri PP, Regehr WG (1996) Determinants of the time course of facilitation at the granule cell to Purkinje cell synapse. J Neurosci 16:5661–5671.

Blatow M, Caputi A, Burnashev N, Monyer H, Rozov A (2003) Ca²⁺ buffer saturation underlies paired pulse facilitation in calbindin-D28k-containing terminals. Neuron 38:79–88.

Borst JG, Helmchen F, Sakmann B (1995) Pre- and postsynaptic whole-cell recordings in the medial nucleus of the trapezoid body of the rat. J Physiol (Lond) 489:825–840.

Borst JGG, Sakmann B (1996) Calcium influx and transmitter release in a fast CNS synapse. Nature 383:431–434.

Borst JGG, Sakmann B (1998) Facilitation of presynaptic calcium currents in the rat brainstem. J Physiol (Lond) 513:149–155.

Caillard O, Moreno H, Schwaller B, Llano I, Celio MR, Marty A (2000) Role of the calcium-binding protein parvalbumin in short-term synaptic plasticity. Proc Natl Acad Sci USA 97:13372–13377.

Celio MR (1990) Calbindin D-28k and parvalbumin in the rat nervous system. Neuroscience 35:375–475.

Collin T, Chat M, Lucas MG, Moreno H, Racay P, Schwaller B, Marty A, Llano I (2005) Developmental changes in parvalbumin regulate presynaptic Ca²⁺ signaling. J Neurosci 25:96–107.

Cuttle MF, Tsujimoto T, Forsythe ID, Takahashi T (1998) Facilitation of the presynaptic calcium current at an auditory synapse in rat brainstem. J Physiol (Lond) 512:723–729.

Du J, Zhang L, Weiser M, Rudy B, McBain CJ (1996) Developmental expression and functional characterization of the potassium-channel subunit Kv3.1b in parvalbumin-containing interneurons of the rat hippocampus. J Neurosci 16:506–518.

Eberhard M, Erne P (1994) Calcium and magnesium binding to rat parvalbumin. Eur J Biochemistry 222:21–26.

Edmonds B, Reyes R, Schwaller B, Roberts WM (2000) Calretinin modifies presynaptic calcium signaling in frog saccular hair cells. Nat Neurosci 3:786–790.

Felmy F, Schneggenburger R (2004) Developmental expression of the Ca²⁺-binding proteins calretinin and parvalbumin at the calyx of held of rats and mice. Eur J Neurosci 20:1473–1482.

Felmy F, Neher E, Schneggenburger R (2003) Probing the intracellular calcium sensitivity of transmitter release during synaptic facilitation. Neuron 37:801–811.

Forsythe ID (1994) Direct patch recording from identified presynaptic terminals mediating glutamatergic EPSCs in the rat CNS, in vitro. J Physiol (Lond) 479:381–387.

Grynkiewicz G, Poenie M, Tsien RY (1985) A new generation of Ca2+ indicators with greatly improved fluorescence properties. J Biol Chem 260:3440–3450.

Habets RLP, Borst JGG (2006) An increase in calcium influx contributes to post-tetanic potentiation at the rat calyx of Held synapse. J Neurophysiol 96:2868–2876.

Haiech J, Derancourt J, Pechere JF, Demaille JG (1979) Magnesium and calcium binding to parvalbumins: evidence for differences between parvalbumins and an explanation of their relaxing function. Biochemistry 18:2752–2758.

Helmchen F, Borst JGG, Sakmann B (1997) Calcium dynamics associated with a single action potential in a CNS presynaptic terminal. Biophys J 72:1458–1471.

Jackson M, Redman S (2003) Calcium dynamics, buffering, and buffer saturation in the boutons of dentate granule-cell axons in the hilus. J Neurosci 23:1612–1621.

Kim J, Alger BE (2001) Random response fluctuations lead to spurious paired-pulse facilitation. J Neurosci 21:9608–9618.

Lee SH, Schwaller B, Neher E (2000) Kinetics of Ca²⁺ binding to parvalbumin in bovine chromaffin cells: implications for $[Ca^{2+}]$ transients of neuronal dendrites. J Physiol (Lond) 525:419–432.

Lohmann C, Friauf E (1996) Distribution of the calcium-binding proteins parvalbumin and calretinin in the auditory brainstem of adult and developing rats. J Comp Neurol 367:90–109.

Macica CM, von Hehn CA, Wang LY, Ho CS, Yokoyama S, Joho RH, Kaczmarek LK (2003) Modulation of the kv3.1b potassium channel isoform adjusts the fidelity of the firing pattern of auditory neurons. J Neurosci 23:1133–1141.

Martina M, Schultz JH, Ehmke H, Monyer H, Jonas P (1998) Functional and molecular differences between voltage-gated K⁺ channels of fast-spiking interneurons and pyramidal neurons of rat hippocampus. J Neurosci 18:8111–8125.

Matveev V, Zucker RS, Sherman A (2004) Facilitation through buffer saturation: constraints on endogenous buffering properties. Biophys J 86:2691–2709.

Mennerick S, Zorumski CF (1995) Paired-pulse modulation of fast excitatory synaptic currents in microcultures of rat hippocampal neurons. J Physiol (Lond) 488:85–101.

Meyer AC, Neher E, Schneggenburger R (2001) Estimation of quantal size and number of functional active zones at the calyx of held synapse by nonstationary EPSC variance analysis. J Neurosci 21:7889–7900.

Nägerl UV, Novo D, Mody I, Vergara JL (2000) Binding kinetics of calbindin-D$_{28k}$ determined by flash photolysis of caged Ca^{2+}. Biophys J 79:3009–3018.

Neher E (1998) Usefulness and limitations of linear approximations to the understanding of Ca^{++} signals. Cell Calcium 24:345–357.

Neher E, Augustine GJ (1992) Calcium gradients and buffers in bovine chromaffin cells. J Physiol (Lond) 450:273–301.

Pór A, Pocsai K, Rusznák Z, Szücs G (2005) Presence and distribution of three calcium binding proteins in projection neurons of the adult rat cohlear nucleus. Brain Res 1039:63–74.

Rudy B, McBain CJ (2001) Kv3 channels: voltage-gated K$^+$ channels designed for high-frequency repetitive firing. Trends Neurosci 24:517–526.

Schmidt H, Brown EB, Schwaller B, Eilers J (2003a) Diffusional mobility of parvalbumin in spiny dendrites of cerebellar Purkinje neurons quantified by fluorescence recovery after photobleaching. Biophys J 84:2599–2608.

Schmidt H, Stiefel KM, Racay P, Schwaller B, Eilers J (2003b) Mutational anaylsis of dendritic Ca^{2+} kinetics in rodent Purkinje cells: role of parvalbumin and calbindin D$_{28k}$. J Physiol (Lond) 551:13–32.

Schneggenburger R (2004) Ca^{2+} uncaging in nerve terminals. In: Imaging in neuroscience and development (Yuste R, Konnerth A, eds).

Schneggenburger R, Meyer AC, Neher E (1999) Released fraction and total size of a pool of immediately available transmitter quanta at a calyx synapse. Neuron 23:399–409.

Schwaller B, Dick J, Dhoot G, Carroll S, Vrbova G, Nicotera P, Pette D, Wyss A, Bluethmann H, Hunziker W, Celio MR (1999) Prolonged contraction-relaxation cycle of fast-twitch muscles in parvalbumin knockout mice. Am J Physiol 276:C395–C403.

Tsujimoto T, Jeromin A, Saitoh N, Roder JC, Takahashi T (2002) Neuronal calcium sensor 1 and activity-dependent facilitation of P/Q-type calcium currents at presynaptic nerve terminals. Science 295:2276–2279.

Vreugdenhil M, Jefferys JG, Celio MR, Schwaller B (2003) Parvalbumin-deficiency facilitates repetitive IPSCs and gamma oscillations in the hippocampus. J Neurophysiol 89:1414–1422.

Wang L-Y, Gan L, Forsythe ID, Kaczmarek LK (1998) Contribution of the Kv3.1 potassium channel to high-frequency firing in mouse auditory neurones. J Physiol (Lond) 509:183–194.

Xu J, Wu LG (2005) The decrease in the presynaptic calcium current is a major cause of short-term depression at a calyx-type synapse. Neuron 46:633–645.

Xu T, Naraghi M, Kang H, Neher E (1997) Kinetic studies of Ca^{2+} binding and Ca^{2+} clearance in the cytosol of adrenal chromaffin cells. Biophys J 73:532–545.

Zhou Z, Neher E (1993) Mobile and immobile calcium buffers in bovine adrenal chromaffin cells. J Physiol 469:245–273.

Zucker RS, Regehr WG (2002) Short-term synaptic plasticity. Annu Rev Physiol 64:355–405.